Pergamon

Geochimica et Cosmochimica Acta, Vol. 67, No. 13, pp. 2497–2507, 2003

0016-7037/03 $30.00 + .00

doi:10.1016/S0016-7037(02)01349-2

Magmatic fractionation of Hf and W: Constraints on the timing of core formation and differentiation in the Moon and Mars

K. RIGHTER[1,*] and C. K. SHEARER[2]

[1]Lunar and Planetary Laboratory, University of Arizona, Tucson, AZ 85721-0092, USA
[2]Institute of Meteoritics, Department of Earth and Planetary Sciences, University of New Mexico, Albuquerque, NM 87122, USA

(*Received February* 4, 2002; revised 6 November 2002; *accepted in revised form November* 6, 2002)

Abstract—Excesses of ^{182}W have previously been measured in samples from the Moon and Mars, and can be derived from high Hf/W regions in their interiors during their early histories. Although planetary mantles will have superchondritic Hf/W after core formation, the extent to which high Hf/W regions could be generated by magmatic fractionation has not been evaluated. In order to address the latter possibility, we have carried out experiments from 100 MPa to 10.0 GPa, 1150 to 1850°C, at oxygen fugacities near the IW (iron-wüstite) buffer, and measured partition coefficients for W and Hf for plagioclase-liquid, olivine-liquid, orthopyroxene-liquid, clinopyroxene-liquid, garnet-liquid, and metal-liquid pairs. Clinopyroxene and garnet are both capable of fractionating Hf from W during magmatic crystallization or mantle melting, and minor variations in the measured *D*'s can be attributed to crystal chemical effects. Excesses of ^{182}W and ^{142}Nd in lunar samples can be explained by fractionation of Hf from W, and Sm from Nd (by ilmenite and clinopyroxene) during crystallization of the latest stages of a lunar magma ocean. Correlations of ε_W with ε_{Nd} in martian samples could be a result of early silicate fractionation in the martian mantle (clinopyroxene and/or garnet).

1. INTRODUCTION

Rocky planets are differentiated into metallic cores and silicate mantles. The timing of such differentiation has until recently been relatively unconstrained. Short-lived isotopes such as ^{182}Hf, ^{146}Sm, ^{60}Fe and ^{26}Al, can offer constraints on the timing of differentiation events that occurred within the lifetime of the parent isotopes (Carlson and Lugmair, 2000). In particular, the decay of ^{182}Hf to ^{182}W, with a half life of 9 Ma, can place constraints on the timing of differentiation up to ~60 Ma after T_0. Isotopic enrichments of ^{182}W, compared to terrestrial standards, have been measured in both lunar and martian materials, and suggest that the Moon formed between 30 and 55 Ma after T_0 and Mars formed ~15 Ma after T_0 (Lee and Halliday, 1997; Lee et al., 1997, 2002; Kleine et al., 2002; Schoenberg et al., 2002; Yin et al., 2002). This ^{182}W isotopic signature may have its origin from several processes: (1) cosmogenic production at the lunar or martian surface, (2) early Hf-W fractionation during core formation that was preserved in the lunar or martian mantle, and (3) early Hf-W fractionation during lunar or martian magma ocean crystallization that was preserved in cumulates. Although a cosmogenic ^{182}W isotopic signature has been detected in lunar samples (Leya et al., 2000), many samples have an excess of ^{182}W compared to terrestrial standards (Lee et al., 2001).

The Hf-W system is of particular interest because Hf is lithophile—remaining in the mantle after core formation—and W is siderophile—being extracted mainly into the metallic core. As a result, high Hf-W ratios in the mantle lead to production of ^{182}W that can constrain the timing of core formation and mantle differentiation. Because of this dual behavior, Hf and W must be studied in both metal-bearing and metal-free systems. The former has been well characterized in studies of *D*(W) metal/silicate (e.g., Palme and Rammensee, 1981; Newsom and Drake, 1982; Ertel et al., 1996; Jaeger and Drake, 2000). Although Hf partitioning in metal-free silicate systems is well known, due to applications to the Lu-Hf isotope system (e.g., Patchett, 1983), W partitioning in silicate systems remains poorly characterized. We know that W is similar in incompatibility to U from correlated trace element analysis of lunar and terrestrial samples (Palme and Wanke, 1975; Newsom et al., 1996). But knowledge of W partition coefficients for specific phases would be of great interest and utility in interpreting W isotopic data.

In this study, we investigate the partitioning behavior of Hf and W between a variety of deep mantle and magmatic silicates and silicate melts. Using these new results, we evaluate the role of magmatic fractionation in generating W isotopic signatures observed in lunar rocks and Martian meteorites and speculate about the early differentiation of the Moon and Mars.

2. EXPERIMENTAL-ANALYTICAL APPROACH

Experiments were conducted in a 0.5-inch non end-loaded piston cylinder apparatus and Walker-style multi-anvil press at the University of Arizona. Piston cylinder experiments were done at 1.0 to 1.5 GPa; multi-anvil experiments were done between 4.0 and 10.0 GPa using WC cubes with 8-mm truncated edge lengths. Pressure in the latter assemblies was calibrated against the quartz-coesite (3.1 GPa), fayalite-spinel (5.75 GPa), and coesite-stishovite (9.3 GPa) transitions at 1200°C (see Righter and Drake, 2000).

Four silicate compositions were selected according to their liquidus phases at various pressures and temperatures: a calc-

* Author to whom correspondence should be addressed (righter@lpl.arizona.edu).
Current address: Kevin Righter, Mailcode St, NASA Johnson Space Center, 2101 NASA Rd. One, Houston, TX 77058, (kevin.righter-1@nasa.gov).

Table 1. Starting compositions used in this study.

	A	B	C	D	E	F
SiO_2	39.99	43.66	50.0	50.79	34.23	46.3
TiO_2	3.56	2.97	—	1.10	0.15	3.12
Al_2O_3	11.44	13.13	13.0	16.57	3.27	16.6
Fe_2O_3	14.16	—	—	0.41	—	4.00
FeO	—	14.84	19.0	7.46	27.15	7.45
MnO	0.21	0.21	—		0.18	0.17
MgO	9.49	9.75	7.0	8.87	24.62	7.1
CaO	11.17	12.12	11.0	9.34	2.61	8.98
Na_2O	3.39	2.5	—	3.32	0.45	3.35
K_2O	0.91	0.86	—	1.83	0.03	1.50
P_2O_5	1.76	0.37	—	0.33	0.23	0.55
LOI	4.07	—	—	—	—	—
Total	100.15	101.15	100.0	100.02	99.98*	99.12

A) Castle Butte monchiquite (Alibert et al., 1986), B) H65-14, ankaramite (Chen et al., 1990), C) synthetic eucrite basalt (Newsom and Drake, 1982), D) 542, subalkaline basalt (Hasenaka and Carmichael, 1987), E) Allende CV3 carbonaceous chondrite (Jarosewich, 1990; * total includes other elements such as Ni, C, S and Cr). F) 14, alkali basalt (Righter and Carmichael, 1993).

alkaline basalt for olivine-, augite- and plagioclase-liquid equilibrium, two alkali basalts (ankaramite and monchiquite) for garnet-liquid and pyroxene-liquid equilibrium, and a synthetic eucrite basalt for orthopyroxene-liquid, and garnet-liquid equilibrium (Table 1). In particular, the liquidus clinopyroxene for each composition is different such that the effect of CaO contents of clinopyroxene on *D*(Hf) and *D*(W) could be evaluated. Each composition was doped with ~0.5 wt.% WO_3 and/or HfO_2, and most were encapsulated with graphite-lined Pt tubing of 0.12-inch diameter. The graphite lining minimizes or eliminates loss of Fe to the Pt capsules, and also buffers fO_2 close to that of the C-CO-CO_2 equilibrium (e.g., Holloway et al., 1992). Several additional experiments for metal-silicate partitioning utilized chondritic and alkali basalt compositions (Table 1), doped with Ni, Co, and W, and encapsulated with MgO or graphite (Table 2).

Neither Hf nor W is multivalent (Ertel et al., 1996, show that W is 4+), and thus their partitioning behavior is not likely to be dependent upon fO_2. However, because some phases such as clinopyroxene and garnet can incorporate significant amounts of Fe_2O_3, it was important to complete these experiments at the reducing conditions appropriate for the Moon and Mars, where most of the oxidized iron is stable as FeO. Oxygen fugacity was measured in eight different runs (Table 3), by use of a mixture of Co metal and CoO-MgO where the oxide composition is a sliding fO_2 sensor (Taylor et al., 1992). The fO_2 of these runs, between 1.0 and 1.5 GPa and 1150 to 1300°C, was close to that of the iron-wüstite buffer (IW to IW + 2), and thus relevant to the reducing conditions present in the early lunar and martian mantles (Righter and Drake, 1996; Wadhwa, 2001; Herd et al., 2002). Several runs were done at lower fO_2's where metal is stable, allowing calculation of oxygen fugacity using the equilibrium $Fe + 1/2O_2 = FeO$, as outlined by Righter et al. (1997). Using this approach, experiment 54 (Table 2) at 1300°C, equilibrated at a $\log fO_2$ of −10.23, 0.39 $\log fO_2$ units above the IW buffer. Experiment 9b, from the study of Newsom and Drake (1982), equilibrated at a $\log fO_2$ of −13.4, 1.4 $\log fO_2$ units below the IW buffer. Oxygen fugacity for the four metal-

Table 2. Experimental run conditions.

Run	*P* (GPa)	*T* (°C)	Duration (h)	Comp.[a]	Fo/Fo_{pred}[b]	Capsule	Dopants	Phases
9b[c]	100 MPa	1190	288	C	—	Al_2O_3	W	opx, plag, gl
54	1.0	1300	4	C	—	KOVAR	W	oliv, gl
133	1.0	1250	21	C	—	Pt (C)	W	oliv, cpx, pl, gl
134	1.95	1275	23	C	—	Pt (C)	W	gt, gl
139	1.0	1125	24	D	—	Pt (C)	W	pig, gl
147	1.5	1300	24	B	78/80	Pt (C)	W, Hf	oliv, cpx, gl
148	1.5	1300	24	A	73/77	Pt (C)	W, Hf	cpx, gl
150	1.5	1300	20.5	D	—	Pt (C)	W, Hf	cpx, gl
151	1.5	1250	23	C	—	Pt (C)	W, Hf	cpx, opx, gt, gl
153	5.0	1675	0.75	B	—	Pt (C)	W, Hf	cpx, gt, gl
172	4.0	1575	1.6	B	—	Pt (C)	W, Hf	cpx, gt, gl
107	10.0	1850	0.15	E	91/88	MgO	W	metal, ol, gl
108	5.0	1630	0.5	E	91/95	MgO	W	metal, ol, gl
113	7.0	1700	0.5	F	—	C	W	metal, gt, cpx, gl
116	5.0	1550	0.75	F	—	C	W	metal, gl

gl = glass, gt = garnet, cpx = clinopyroxene, opx = orthopyroxene, oliv = olivine, plag = plagioclase; pig = pigeonite.
[a] Starting compositions from Table 1.
[b] Fo_{pred} refers to the olivine composition predicted by Snyder and Carmichael (1992); Fo = forsterite mol.%.
[c] From Newsom and Drake (1982).

Table 3. Fugacity sensor data and results.

Run #	P (GPa)	T (°C)	n	MgO (wt.%)	CoO (wt.%)	X CoO	fO_2	Δ IW
133	1.0	1250	8	91.5	8.7	0.048	–10.48	0.45
136	1.0	1200	7	50.0	42.6	0.314	–9.55	1.98
137	1.0	1150	3	91.8	9.6	0.053	–11.51	0.65
138	1.0	1175	6	75.8	26.8	0.16	–10.33	1.51
140	1.0	1230	7	84.2	14.9	0.087	–10.2	0.96
144	1.0	1270	12	43.7	54.8	0.403	–8.625	2.08
145	1.0	1400	12	58.6	39.3	0.265	–7.689	1.67
147	1.5	1300	12	93.9	5.9	0.033	–10.03	0.17

n = number of averaged analyses of the oxide. fO_2 calculated using the approach of Taylor et al. (1992) for Co-(Co,Mg)O equilibria: ΔIW is the oxygen fugacity of each experiment relative to the value of the IW buffer (Myers and Eugster, 1983) at the same P and T.

silicate experiments (Table 1) was calculated in the same manner as Righter and Drake (1999) and are tabulated in Table 4.

Phases produced in all experimental charges were analyzed using a Cameca SX-50 electron microprobe. Operating conditions for silicate and metal were 15 kV accelerating potential, 30 nA sample current, and 10-s count times (Si, Ti, Al, Fe, Mg, Ca, Na, K, P, W in silicates; Fe, Ni, Co, S and W in metals). Standards included both natural (diopside, albite, fayalite, apatite, potassium feldspar, troilite) and synthetic (Ni- and Co-diopside glass, iron, cobalt and nickel metals) materials. PAP φ–ρ–z corrections (as supplied by Cameca software) were applied to all analyses. All solid phases and glasses were analyzed with a point beam. Silicate melts in experiments 107 and 108 did not quench to a glass, but rather to a mat of quench crystals; a rastered beam with an area of 25 to 30 μm^2 was used for these samples. Equilibrium was monitored in experiments by measuring olivine-liquid MgO-FeO *Kd*'s (Table 2); comparison to previous studies indicates equilibrium was attained in these runs.

Tungsten and hafnium were measured in the crystalline and glass phases using the Cameca ims 4f operated on the University of New Mexico campus by a UNM–Sandia National Laboratories consortium. Analyses were made using primary O^- ions accelerated through a nominal potential of 12.5 kV. A primary beam current of 25 nA was focused on the sample over a spot diameter of 20 μm. Sputtered secondary ions were energy filtered using a sample offset voltage of 120 V and an energy window of ±50 V. Potential interferences were identified using a mass scan across both Hf and W (Fig. 1). Initial analyses involved repeated cycles of peak counting on ^{182}W, ^{184}W, ^{186}W and ^{30}Si. The analytical procedure included counting on a background position to monitor detection noise. Absolute concentrations of each element were calculated using empirical relationships of $W/^{30}Si^+$ ratios (normalized to known SiO_2 content) to element concentrations as derived from daily calibration. A calibration curve was constructed using a series of W-bearing glasses synthesized in the lab (Fig. 2) and analyzed independently using the electron microprobe (Table 5). Determination of W in individual mineral phases assumes that ionization efficiency is the same as the glass standards. Additional studies evaluating this assumption are currently being made.

3. RESULTS

Partition coefficients for W and Hf in garnet-melt, olivine-melt, orthopyroxene-melt, clinopyroxene-melt, plagioclase-melt pairs, and for W in metal-melt pairs were measured (Table 6) in 12 different experimental runs. Olivine-, orthopyroxene-, and plagioclase-melt D's are <0.08 for Hf and W, and thus magmatic fractionation of these phases cannot produce high Hf/W cumulates. Clinopyroxene and garnet, however, have D's between 0.1 and 1 for Hf, and much lower D's for W, indicating that these two phases can significantly concentrate Hf, fractionate Hf from W, and therefore produce high Hf/W regions in the mantle. Melts generated in a garnet or clinopyroxene-bearing mantle will have a correspondingly lower Hf/W ratio.

Clinopyroxene can contain variable amounts of Na, Ca and Al(vi), and all three of these elements will affect the sizes of octahedral sites, upon which Hf and W are sited. The results of this study can be understood in terms of clinopyroxene composition. Comparison of our new D(Hf) with previous work shows a positive correlation with Al(vi) and Ca contents (Fig. 3), and a negative correlation with Na. Comparison of our new D(W) results with previous work (Hill et al., 2000) shows a negative correlation with Ca and Al. As a result of these differences between D(W) and D(Hf) with crystal chemical changes, D(Hf)/D(W) is highest for CaAl clinopyroxenes, and

Table 4. Electron microprobe analyses of metal.

Run #	n	ΔIW	Fe	Ni	Co	W	S	C	P	Total
107	8	−0.52	56.77	16.10	12.54	2.51	8.54	—	0.15	96.60
108	7	−1.79	56.40	18.55	12.49	0.63	8.27	—	0.02	96.36
113	3	−1.16	51.35	17.40	14.45	1.51	8.05	—	0.08	92.83
116	6	−2.20	72.90	0.16	0.26	13.68	0.51	—	1.64	89.17

n = number of averaged analyses of the metal. fO_2 calculated using the approach of Righter et al. (1997): ΔIW is the oxygen fugacity of each experiment relative to the value of the IW buffer (Myers and Eugster, 1983) at the same P and T.

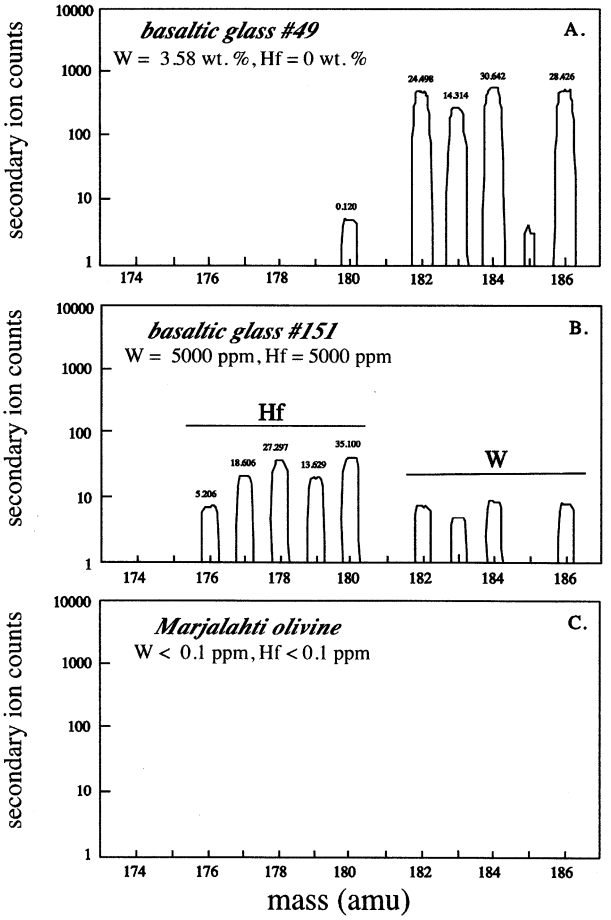

Fig. 1. Mass scans for W (A) and Hf (B) isotopes on experimental glasses 49 (from Righter and Drake, 1999) and 151. Also shown is a mass scan across the Marjalahti pallasite olivine (C).

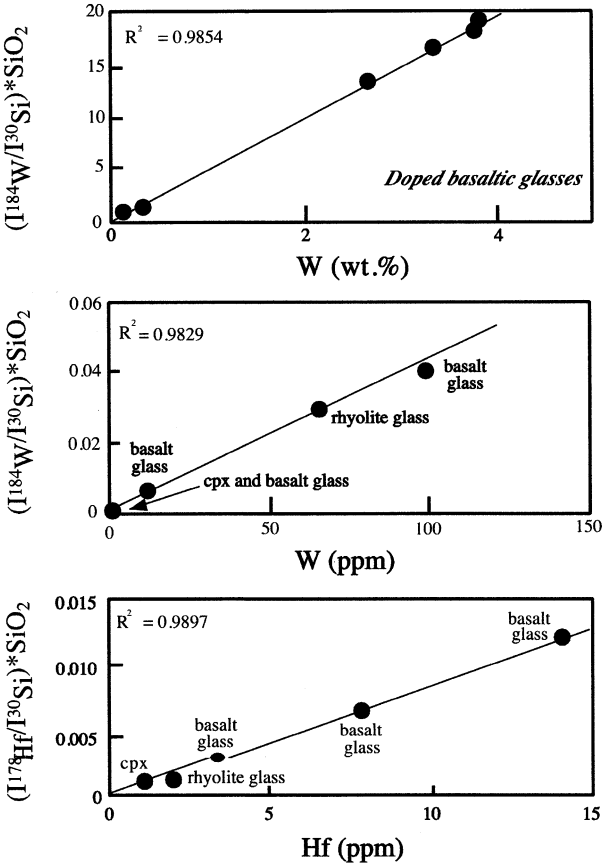

Fig. 2. Ion microprobe calibration curve for W and Hf in silicate glass. W-bearing glasses were synthesized in 1-bar experiments doped with W, and were analyzed by electron microprobe (Table 5).

is decreased by the jadeite component. The implications of this crystal chemical dependence will be discussed below, but it is clear that any discussion of Hf/W fractionation must first specify a clinopyroxene composition.

Partitioning of many incompatible elements between garnet and liquid has been shown to be dependent upon the Ca content, or grossular component, of the garnet (e.g., van Westrenen et al., 1999, 2001). Comparison of our new results for *D*(Hf) to those published previously confirm this dependence (Fig. 4), as there is a negative correlation between X_{Ca} and *D*(Hf). Our new results for *D*(W) garnet/melt are the first, preventing comparison to previous results (Fig. 4). The large differences between *D*(Hf) and *D*(W) show that garnet is easily capable of fractionating Hf from W. In fact, pyrope-rich garnets, those applicable to the lunar, terrestrial or martian mantles, will fractionate Hf from W greater than grossular-rich.

4. DISCUSSION

4.1. Fractionation of Hf From W: Summary and Integration With Metal-Silicate Partitioning

4.1.1. Fractionation due to core formation

The siderophile behavior of W compared to the lithophile behavior of Hf gives this chronometer unusual leverage on constraining the timing of core formation. An understanding of how the Hf/W ratio can be fractionated by core formation or metal-silicate equilibrium is a requirement for any interpretation of subsequent silicate or magmatic fractionation, because the mantle Hf/W ratio will be set by core formation. Mantle Hf/W ratios resulting from core formation depend upon several factors: the initial Hf/W ratio of the bulk planet, core size, and the magnitude of the metal-silicate partition coefficient.

Despite their diverse compositions, chondritic materials have a somewhat restricted range of Hf/W ratios, from 1.02 to 1.55 (from compilation of Newsom, 1995). Therefore, the assumption is that any chondritic material serving as a planetary building block will start out with a Hf/W value somewhere close to 1.

Metallic cores in rocky bodies are variable in size. A large core such as the Earth's will harbor a large portion of a planet's siderophile element budget, whereas a small core such as the Moon's will have a small to negligible effect on the Hf/W ratio of it's mantle. The Hf/W ratio of the mantle Mars, which has a core of intermediate size (~20%) will be affected only marginally by core formation.

Metal/silicate partitioning of W and other siderophile elements is a function of several thermodynamic intensive variables. Temperature, pressure, the fugacities of oxygen and sulfur, and silicate melt composition all affect the magnitude of

Table 5. Electron microprobe analyses of SIMS calibration glasses and silicate phases from run products (wt.%).

Sample	SiO_2	TiO_2	Al_2O_3	FeO	MnO	MgO	CaO	Na_2O	K_2O	P_2O_5	NiO	CoO	HfO_2	WO_2	*n*	Total
cal1 (10)	49.40	—	7.03	29.33	—	7.57	3.97	—	—	—	—	—	—	1.02	3	98.59
cal2 (15)	40.99	—	10.92	30.33	—	3.01	8.54	—	—	—	—	—	—	3.37	5	98.04
cal3 (33)	40.46	—	9.16	31.39	—	5.89	8.06	—	—	—	—	—	—	2.65	5	98.28
cal4 (9b)	55.18	—	15.95	15.19	—	6.67	7.56	—	—	—	—	—	—	0.15	10	100.55
54 gl	25.5	—	9.33	43.32	—	1.15	8.84	—	—	—	0.016	0.18	—	4.83	10	96.09[a]
54 oliv	31.38	—	0.06	60.44	—	7.97	0.46	—	—	—	0.069	0.58	—	n.d.	5	100.96
133 gl	50.76	2.27	17.52	9.35	0.16	3.92	6.35	2.73	3.62	1.27	—	0.08	—	—	9	98.06
133 oliv	38.07	0.08	0.17	24.58	0.29	37.38	0.36	0.04	0.05	0.08	—	0.22	—	—	6	101.33
133 cpx	50.74	0.65	6.51	6.05	0.17	18.46	16.29	0.52	0.02	0.03	—	0.04	—	—	6	100.23
133 pl	55.04	0.09	28.21	0.29	—	0.09	10.22	4.98	1.04	0.03	—	0.03	—	—	9	100.06
134 gl	54.83	0.18	16.75	7.95	0.08	5.32	11.27	0.07	0.02	—	0.43	—	—	0.22	10	97.17
134 gl	39.70	0.07	22.80	16.44	0.16	11.88	9.09	—	—	—	0.84	—	—	—	10	101.29
139 gl	51.82	—	15.26	15.60	0.04	4.09	10.95	0.05	0.02	—	0.84	—	—	—	8	98.71
139 pig	49.01	—	3.76	18.75	0.07	14.44	7.57	0.02	0.01	—	5.00	—	—	—	8	98.67
107 gl[a]	41.29	1.39	9.15	15.01	—	19.59	7.97	—	—	—	0.08	0.30	—	0.95	25	96.38
107 oliv	39.70	n.d.	0.22	8.97	—	48.72	0.32	—	—	—	0.11	0.32	—	n.d.	5	98.55
108 gl[a]	34.84	0.15	7.35	9.93	—	36.42	8.30	—	—	—	0.10	0.25	—	0.37	5	98.77
108 oliv	40.82	n.d.	0.39	8.31	—	49.61	0.61	—	—	—	0.13	0.31	—	n.d.	8	100.39
113 gl	52.23	4.33	10.10	10.24	0.17	4.28	8.20	7.04	0.67	0.15	0.15	0.39	—	0.03	5	98.00
113 gt	40.03	1.73	21.93	16.41	0.62	9.91	9.05	0.71	0.05	—	—	0.36	—	—	7	101.01
113 cpx	53.76	1.31	15.24	5.33	0.16	6.28	8.82	7.53	0.40	—	—	—	—	—	6	98.89
116 gl	47.32	3.39	16.85	10.29	—	6.81	9.12	3.53	1.08	0.53	n.d.	n.d.	—	0.06	15	99.00
147 gl	42.28	3.74	13.40	12.83	0.20	8.06	8.72	3.16	1.48	0.61	n.d.	0.43	1.39	1.59	15	97.94
147 ol	38.12	0.05	0.04	20.80	0.26	40.94	0.30	0.15	0.06	0.03	0.08	1.47	n.d.	n.d.	8	102.43
147 cpx	47.74	1.68	9.32	7.82	—	13.92	16.91	1.15	0.01	0.04	—	0.36	n.d.	n.d.	15	98.92
148 gl	39.29	4.40	13.42	13.59	0.19	6.53	9.05	4.41	2.60	2.25	n.d.	n.d.	1.17	0.51	15	97.47
148 ol	37.98	0.11	0.08	24.55	—	36.62	0.45	0.05	—	0.08	—	0.028	n.d.	n.d.	15	99.95
148 cpx	45.96	3.09	10.71	6.45	—	11.73	20.26	1.35	0.01	0.053	—	—	n.d.	n.d.	15	99.61
151 gl	51.44	0.02	16.41	12.59	0.04	3.57	10.85	0.10	0.03	n.d.	0.75	n.d.	0.65	1.47	15	97.95
151 opx	46.78	0.01	8.53	20.19	0.06	15.47	1.84	0.02	n.d.	n.d.	8.59	n.d.	n.d.	n.d.	8	101.58
151 cpx	48.00	n.d.	8.12	16.82	0.06	11.70	12.04	0.04	n.d.	n.d.	4.56	n.d.	0.10	n.d.	9	101.46
151 gt	38.85	0.04	22.66	21.67	0.11	9.40	6.66	—	—	—	1.06	—	—	—	10	100.53
153 gl	43.17	2.90	11.32	13.64	0.18	11.96	10.31	3.18	1.11	0.35	n.d.	n.d.	1.14	0.46	13	99.79
153 cpx	51.45	0.86	9.48	5.97	0.11	15.00	15.73	2.52	0.04	n.d.	n.d.	n.d.	0.21	n.d.	9	101.54
153 gt	38.03	3.43	17.92	14.58	0.34	14.12	10.01	0.30	n.d.	0.22	n.d.	n.d.	2.17	0.03	8	101.25
172 gl	38.55	4.44	7.87	18.85	0.21	10.61	8.78	4.31	2.04	0.63	n.d.	n.d.	1.53	1.16	15	99.04
172 cpx	52.41	0.82	8.24	6.39	—	13.75	14.81	2.96	0.05	0.02	—	—	0.19	—	10	99.64
172 gl	40.02	1.48	21.16	12.49	0.27	15.15	9.39	0.23	n.d.	0.09	n.d.	n.d.	1.33	0.06	5	101.96

[a] Did not quench to a glass, but to a dendritic mixture of quench crystals: standard deviations for all elements are typically 2% or less.

D(W) metal/silicate. Determination of metal/silicate partition coefficients at high pressures and temperatures has been the focus of many studies in the last 10 yr, resulting in a more comprehensive understanding of siderophile element behavior in planets (e.g., Walter et al., 2000). In particular, the effects of *T*, *P*, oxygen fugacity, silicate melt composition and S- and C-content of the metallic liquid on metal/silicate partition coefficients have been parameterized (Righter et al., 1997; Righter and Drake, 1999). Expressions of the form

$$\ln D(M) = a\ln fO_2 + b/T + cP/T + d\ln(1-X_S) + e\ln(1-X_C) + \sum f_i X_i + g \quad (1)$$

have been derived for W and other siderophile elements (Righter and Drake, 1999). The term $\Sigma f_i X_i$ represents the effect of silicate melt composition in terms of oxide mole fractions (X), and the form follows from the partial molal excess free energy of a multicomponent regular solution (using Ni as an example): $G^{xs} = RT\ln\gamma_{NiO}^{sil.\ melt} = \Sigma X_i W_{iNi} - 1/2\ \Sigma_i\Sigma_j W_{ij}X_iX_j$. A simplified version of this form ($\Sigma f_i X_i$) has the advantage of unravelling effects of particular cations: for instance, opposing effects of two network modifiers such as Mg and Ca (see

Table 6. Summary of partition coefficients.

Phase	Run #	*D*(W)	*D*(Hf)
Olivine	54	0.007–0.02	—
	133	0.0015	—
	147	0.04–0.07	0.07
Low Ca pyroxene	151	0.007–0.015	0.08
	9b	0.025	—
	113	0.012	—
(pigeonite)	139	0.06	—
Hi-Ca pyroxene	151	0.04	0.28
	147	0.18	0.54
	148	0.19	0.56
	133	0.11	—
	172	0.04	0.15
Plagioclase	9b	0.003	—
	133	0.028	—
Garnet	151	0.003	0.52
	153	0.01	0.20
	172	0.01	0.31
	113	0.008	—
	134	0.007	—
Metal	107	2.6	—
	108	1.7	—
	113	50	—
	116	230	—

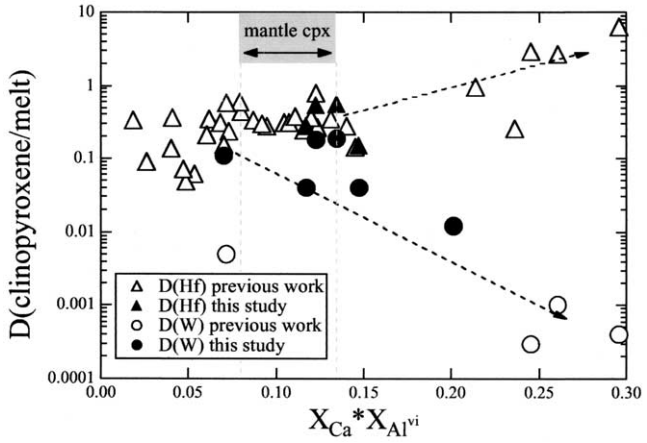

Fig. 3. *D*(Hf) and *D*(W) cpx/liq vs. $X_{ca} \times X_{Al^{vi}}$ from this study (solid symbols) and previous work (open symbols). Previous data for Hf in clinopyroxene are from the studies of Watson et al. (1987), Hill et al. (2000), Skulski et al. (1994), Hauri et al. (1994), Salters and Longhi (1998), Dunn (1987), Hart and Dunn (1993), and Lundstrom et al. (1998). Previous data for W in clinopyroxene are from the study of Hill et al. (2000). Range for mantle clinopyroxene is calculated from spinel peridotite analyses reported by Frey and Prinz (1978).

Righter and Drake, 1999, for a more extensive discussion of this approach). We have combined our new metal-silicate partition coefficients (Table 6) with previous metal-silicate partition coefficient data (Righter and Drake, 1999, and references therein) to derive a new predictive expression for *D*(W) metal-silicate. Coefficients "a" through "g," are tabulated, along with associated error, in Table 7. Using such expressions it is possible to calculate metal/silicate partition coefficients, and resulting mantle W concentrations, for specific conditions within planets or satellites such as the Moon, Mars or Earth.

All of these factors can be combined to quantify the W content and thus the Hf/W ratio of a planetary mantle after core formation. Because both the Moon and Mars are thought have

Table 7. Regression coefficients for *D*(W) metal/silicate.

Variable	Coefficient	Value	1σ
InfO_2	a	–0.99	0.05
1/*T*	b	–64700	3400
P/*T*	c	177	12
X_s	d	6.74	0.80
X_c	e	–7.98	1.42
X_{SiO2}	f	31.6	2.4
X_{Al2O3}	f	18.7	3.1
X_{MgO}	f	14.5	2.1
X_{CaO}	f	16.5	2.8
X_{FeO}	f	15.6	2.5
Constant	g	–6.67	2.50

n = 122; r^2 = 0.942; 2σ error on regression = 1.44.

Data used in the regression are 4 from this study, 9 from Righter and Drake (1999) and 109 experiments utilized in regression of Righter and Drake (1999).

experienced magma oceans early in their history (Righter et al., 1998; Righter, 2002), the following calculations have been simplified for the case of a molten mantle. The concentration of a siderophile element, *M*, in a planet's mantle is (from Hillgren, 1991)

$$C^M_{LS} = \frac{C^M_{bulk}}{[x + (1-x)(D^M_{LM/LS})]} \quad (2)$$

where x = silicate fraction of the planet, C^M_{LS} and C^M_{bulk} are concentrations of *M* in the magma ocean and bulk planet, respectively, and $D^M_{LM/LS}$ is calculated using Eqn. 1. Using this expression, it is possible to calculate the concentration of W and Hf/W in the mantles of Mars and Earth, after core formation (Fig. 5).

4.1.2. Moon

The Moon is a special case because it is thought to be composed of mantle material derived from the impactor during

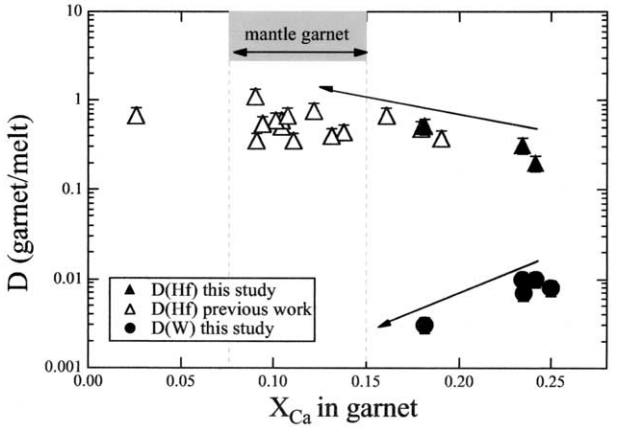

Fig. 4. *D*(Hf) and *D*(W) gt/liq vs. X_{Ca} of garnet from this study (solid symbols) and previous work (open symbols). Previous data for Hf in garnet are from the studies of Hauri et al. (1994), Salters and Longhi (1998), and van Westrenen et al. (1999, 2001). There are no previous data for W in garnet. Range for mantle garnet is calculated from garnet peridotite analyses reported by Nixon (1987).

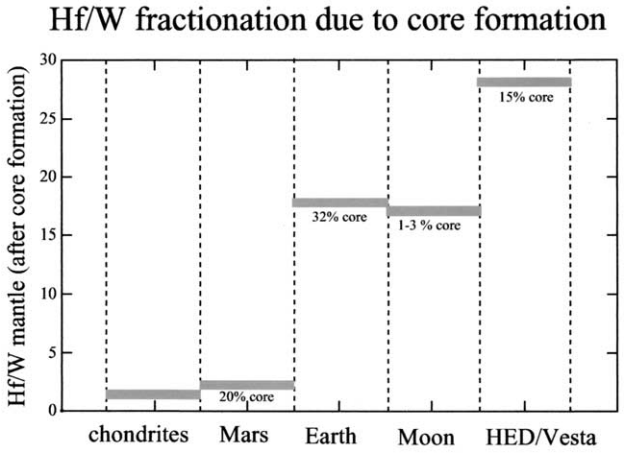

Fig. 5. Hf/W of the primitive mantles of the Moon, Mars, Earth and Vesta (EPB) compared to chondrites. Note the very small Hf/W ratio of the mantle of Mars. Values were taken from Newsom (1995), Righter et al. (1998), Righter and Drake (1996), Newsom et al. (1996), and Dreibus and Wanke (1980).

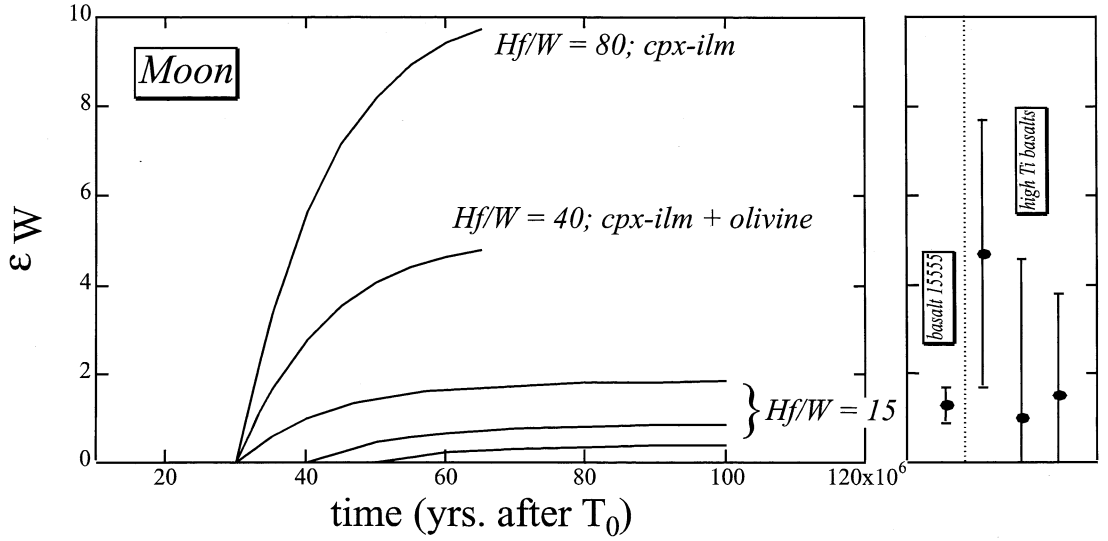

Fig. 6. Evolution of ε_W for different parts of the lunar mantle, using Eqn. 3 in the text. The three low curves are calculated for the lunar mantle after core formation, with Hf/W = 15, and starting at three different times: 30, 40 and 50 Ma after T_0. The highest curve was calculated for a clinopyroxene-ilmenite cumulate, with a Hf/W ratio of 80, and the intermediate curve was calculated for a 50:50 mixture of clinopyroxene-ilmenite cumulate and olivine (after van Orman and Grove, 2000, and Elkins-Tanton et al., 2002), with a Hf/W ratio of 40. Details of Eqn. 3 and values used in the equation are given in the text. Data for lunar samples on the right are from Lee et al. (2002), and are corrected for cosmogenic derived ^{182}W.

an impactor—proto-Earth collision. As a result, the Hf/W ratio of the mantle of the Moon will be set by both core formation in the impactor, and any additional core formation within the extant Moon (e.g., Shearer and Newsom, 2000). The former event will have the largest effect on the Hf/W ratio, as the core size in the impactor is likely to be in the range of 20 to 30%. However, the latter event was most likely followed by formation of a small core (1 to 2%; Hood and Zuber, 2000; Righter, 2002), and elevation of Hf/W due to core formation within the Moon will be very small (Fig. 5). As a result, the Moon's Hf/W ratio is largely inherited from the impactor mantle.

After its rapid formation from an impact generated disk (e.g., Ida et al., 1997), the Moon had an extensive magma ocean (e.g., Warren, 1985; Shearer and Papike, 1999). During crystallization of the magma ocean, garnet, clinopyroxene and ilmenite may have generated regions of high Hf/W in the lunar mantle. Two different scenarios can be considered in terms of the extent of Hf/W fractionation due to mantle differentiation: shallow late-stage crystallization of the magma ocean, and formation of a deep garnet layer.

The last stages of crystallization of the lunar magma ocean (LMO) most likely involved clinopyroxene and ilmenite (e.g., Snyder et al., 1992). Density contrasts, multiple saturation depths and physical modelling for the more primitive mare basalts suggest that these late-stage cumulates were later mixed into the deep mantle source regions of the mare basalts (e.g., Warren, 1985; Snyder et al., 1992; Hess and Parmentier, 1995; Shearer and Papike, 1999). Recent considerations of the kinetics (van Orman and Grove, 2000) and dynamics (Elkins-Tanton et al., 2002) of this scenario suggest that a mixture of clinopyroxene-ilmenite cumulates and olivine would be capable of sinking through the lunar mantle to depths of 200 to 300 km. If the clinopyroxene-ilmenite cumulates formed within the lifetime of ^{182}Hf, later remelting of these mixtures would contain excesses of ^{182}W. Coupling the petrologic constraints with the Hf and W partition coefficients measured in this study, the Hf/W ratio of the resulting clinopyroxene-ilmenite cumulates can be predicted. For clinopyroxene, D(Hf)/D(W) = 5 (Table 6), and for ilmenite, D(Hf)/D(W) = 4 (McKay et al., 1986; McKay and Le, 1999). If a cumulate layer of 67% clinopyroxene–33% ilmenite formed, it would have a Hf/W ratio of 80. Subsequent mixture of this cumulate material in a 50:50 ratio with olivine from the lunar mantle, would result in a Hf/W ratio of 40, or a factor of ~2.7 higher than the lunar mantle after core formation.

The ^{182}W evolution of this mixture in the mantle can then be calculated using Eqn. 3 of Harper and Jacobsen (1996):

$$\varepsilon^{mantle}_{182W}(t) = Q_{182W} \cdot f^{Hf/W}_{mantle} \cdot \left(\frac{^{182}Hf}{^{180}Hf}\right)_{T_0} [e^{-\lambda_{182}(T_0-T_{cf})} - e^{-\lambda_{182}'} \quad (3)$$

where Q_{182W} = 15,500 (from Harper and Jacobsen, 1996), $f^{Hf/W}_{mantle} = \left(\frac{(^{180}Hf/^{183}W)_{mantle}}{(^{180}Hf/^{183}W)_{CHUR}} - 1\right)$, $\left(\frac{^{182}Hf}{^{180}Hf}\right)_{T_0} = 1.0\times10^{-4}$ (from Kleine et al., 2002; Yin et al., 2002; Schoenberg et al., 2002), T_0 = 4.566 Ga, and T_{cf} = 30, 40 and 50 Ma after T_0. The ^{182}W evolution of the lunar mantle for three different lunar formation times—30, 40 and 50 Ma (Fig. 6) —shows that even the oldest age, 30 Ma after T_0, can only produce ε_W value as high as ~+2. The values measured in high Ti basalts, however, are as high as +4.7 (Lee et al., 2002). Rapid remelting of the cumulate or cumulate-olivine mixtures discussed above, on the other hand, could easily produce ε_W values as high as +5 (Fig. 6).

The positive ε_W in the source region of some of the mare basalts is accompanied by positive excesses of ^{142}Nd. This latter isotope is derived from alpha decay of ^{146}Sm, which has

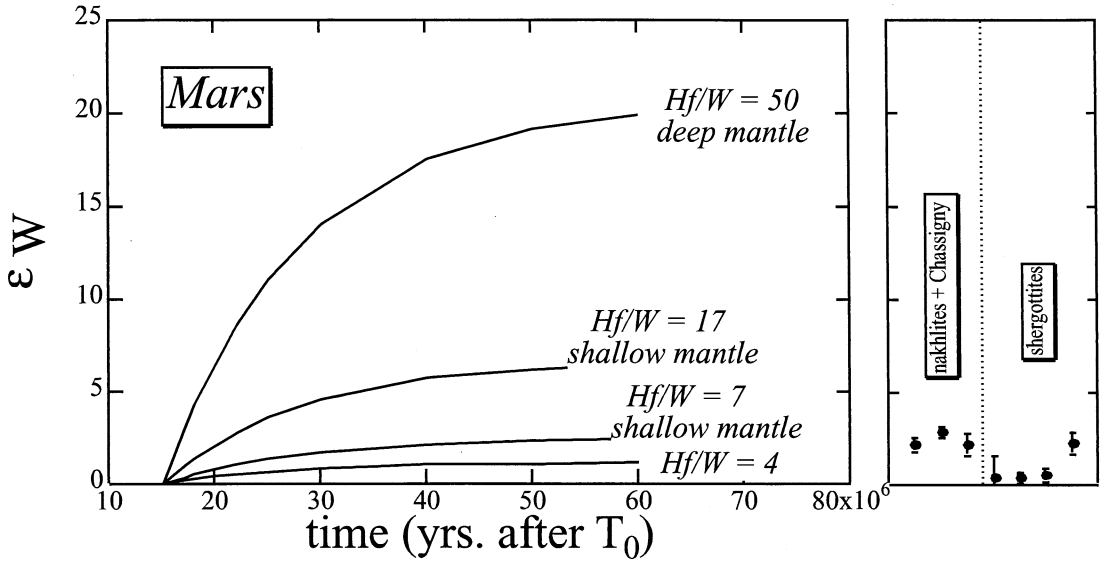

Fig. 7. Evolution of ε_W for different parts of the martian mantle, using Eqn. 3 in the text. The low curve is calculated for the martian mantle after core formation, with Hf/W = 4, and starting at 15 Ma after T_0. The highest curve was calculated for a majorite-bearing (40%) deep mantle, with a Hf/W ratio of 50. The intermediate curves were calculated for a shallow garnet-bearing mantle (Hf/W = 17) and garnet-free mantle (Hf/W = 7). Details of Eqn. 3 and values used in the equation are given in the text. The shallow and deep mineralogy of the martian mantle is taken from the Bertka and Fei (1997) mineralogic model for the interior of Mars. Data for SNC meteorites on right are from Lee and Halliday (1997).

a half-life of 103 Ma. The combination of the ε_W and ^{142}Nd enrichments in lunar samples places further constraints on the timing of differentiation of the lunar mantle and the duration of the crystallization of the LMO. Low Ti basalt sample 15555 has a small positive value of ε_W (1.3 ± 0.39; Lee et al., 2002) and an ε_{142Nd} value that is unresolvable from zero (Nyquist et al., 1995), consistent with derivation from the primitive olivine and orthopyroxene cumulate bearing lunar mantle. On the other hand, sample 75075 has large positive values of ε_W (4.7 ± 3.0; Lee et al., 2002) and ε_{142Nd} (0.29 ± 0.11; Nyquist et al., 1995), consistent with derivation from a clinopyroxene- and ilmenite-rich cumulate layer at depth in the lunar mantle. The magnitude of both high Ti basalt enrichments can best be explained by very rapid crystallization of the LMO, <30 Ma (Fig. 6). This rapid crystallization implies that the very early lunar crust was not as stable and insulating as previously suggested (e.g., Solomon and Longhi, 1977; Spera, 1992). In fact, some have calculated that magma oceans can crystallize as rapidly as 1000 years (Davies, 1990; Solomotov, 2000). Fundamental changes in crustal formation from LMO to serial magmatism processes occurred early in the evolution of the Moon.

4.1.3. Mars

Core formation in Mars is thought to have occurred under high temperature, low pressure and reduced conditions (Righter and Drake, 1996; Righter et al., 1998). The formation of its 20 mass% core, however, resulted in a low mantle Hf/W ratio of 4 (Righter et al., 1998; Halliday et al., 2001). This low value for the martian mantle is not capable of producing the large excesses of ^{182}W measured in some of the SNC meteorites by Lee and Halliday (1997). Using Eqn. 3, a Hf/W ratio of 4, and a core formation time (T_{cf}) of 15 Ma after T_0, values of ε_W only reach ~+1 (Fig. 7). ε_W for the nakhlites, Chassigny and EETA 79001, however, reaches values of >3. As a result, additional fractionation of Hf from W in the mantle is required to explain the latter isotope data.

Although ilmenite is not a relevant phase in martian mantle petrologic models, clinopyroxene and garnet are both stable well into the martian mantle—up to pressures of 16 and 25 GPa, respectively (Longhi et al., 1992; Bertka and Fei, 1997). Using the mantle bulk composition proposed by Longhi et al. (1992), the mineralogy of the martian mantle can be predicted as a function of pressure (Bertka and Fei, 1997). Shallow mantle mineralogy includes clinopyroxene, intermediate mantle mineralogy includes garnet and clinopyroxene, and deep mantle mineralogy includes majorite-rich garnet. Early differentiation of the martian mantle would provide two scenarios in which to generate higher Hf/W ratios than that due to core formation (Fig. 7), and thus contribute to ^{182}W enrichments that have been measured (Lee and Halliday, 1997) in the SNC meteorites: a deep majoritic garnet-bearing mantle and a shallower clinopyroxene and/or garnet bearing mantle.

In the case of a deep garnet-rich mantle, Hf/W ratios could reach values as high as 50, given D(Hf)/D(W) = 30, and a 40% majorite-rich garnet-bearing deep mantle (reported by Bertka and Fei, 1997). Such a mantle would rapidly attain ε_W values as high as 20, within 45 Ma after core formation (Fig. 7). These are far higher than values measured in nakhlites. Although it might be possible to reduce the size of such an excess by mixing between mantle and a low Hf/W reservoir such as the crust over time, Os, Hf and Nd isotopes preclude a major role for such a mixing process (Brandon et al., 2000).

A second, and more likely scenario for generating the excesses of ^{182}W in martian samples is by melting of a

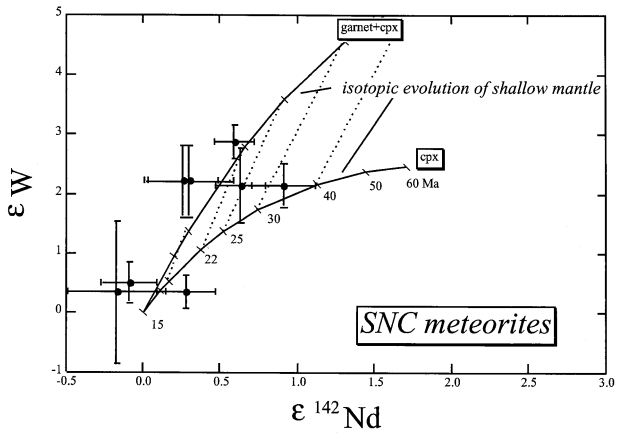

Fig. 8. ε_W vs. ε_{142Nd} for martian meteorite samples (data from Nyquist et al., 1995; Lee and Halliday, 1997). Two curves are shown—the W and Nd isotopic evolution for 1) a martian mantle with 10% garnet and 10% clinopyroxene, and 2) a garnet-free mantle (20% clinopyroxene), both based on the mineralogy of Bertka and Fei (1997). The numbers along the solid lines are millions of years after CAI formation. Most of the isotopic data are consistent with derivation from a garnet-bearing mantle. Dashed lines connect garnet-bearing and garnet-free sources at the same time step. Note that the data for Lafayette and Shergotty fall off the line and require only a small amount of garnet, or simply a clinopyroxene-bearing mantle. Partition coefficients for Sm and Nd for these calculations were the same as used by Borg et al. (1997).

shallow mantle source (that formed early) containing clinopyroxene and/or garnet (Bertka and Fei, 1997). A mantle containing 10% clinopyroxene with $D(\mathrm{Hf})/D(\mathrm{W}) = 5$, and 10% garnet with $D(\mathrm{Hf})/D(\mathrm{W}) = 30$, would have a Hf/W ratio of 17 (Fig. 7). Such a mantle would produce large excesses of ^{182}W within ~20 Ma, with a magnitude similar to those measured in the nakhlites, Chassigny and EETA79001 (Fig. 7). Furthermore, a garnet-free mantle with 20% clinopyroxene would have a Hf/W ratio of 7, and would also evolve large excesses of ^{182}W within ~45 Ma. This scenario is also in agreement with measurements of Os, Nd and Hf isotopes that indicate melting of a garnet-bearing mantle to explain these isotopic data (Borg et al., 1997; Blichert-Toft, et al., 1999; Brandon et al., 2000).

The positive ^{182}W isotope anomalies among the SNC meteorites are coupled with positive ^{142}Nd anomalies (Fig. 8; Harper et al., 1995). The ability of clinopyroxene and garnet to fractionate Sm/Nd as well as Hf/W suggests that these two anomalies are correlated due to control by one or both of these phases early in the history of martian differentiation. Most of the ε_W and ε_{142Nd} values can be explained by simple models involving a garnet-bearing mantle. A few meteorites (Lafayette and Shergotty) can form without the need for garnet fractionation, but small amounts are not ruled out either. In summary, formation of a 20 mass% metallic core, followed by melting of a clinopyroxene and garnet-bearing mantle, all within ~30 Ma of T_0, can reproduce both the ε_W and ε_{142Nd} values measured in the SNC meteorites.

5. SUMMARY AND FUTURE

The new partitioning data reported here, indicating that the phases garnet and clinopyroxene can fractionate Hf from W and produce high Hf/W cumulates or mantle, allow an explanation of ^{182}W excesses measured in lunar and martian samples. Positive ε_W values measured in lunar sample 15555 can be explained by early (30 Ma after T_0) differentiation of the Moon, involving a high Hf/W mantle. Hf/W and Sm/Nd ratios of parts of the mantle were later enhanced by clinopyroxene and ilmenite fractionation in a late magma ocean scenario, leading to even larger positive values of ε_W and ε_{Nd} in the high Ti melts that later formed from such a source. Small, positive ε_W and ε_{Nd} measured in SNC meteorites can be easily explained by early (15 Ma after T_0) core formation and mantle differentiation in Mars, the latter involving garnet and clinopyroxene in the shallow mantle. These scenarios explain the isotope data well, but as new data become available for interpretation, several additional scenarios may be worth evaluating.

Another scenario in which early, high Hf/W regions can be produced in the lunar mantle involves the presence of garnet in the deep, unmelted, primitive lunar mantle. Because garnet can also fractionate Hf from W, and is thus capable of producing high Hf/W ratios, it's potential role in the generation of lunar W isotope enrichments should be discussed. Seismic properties (density profiles) of the deep lunar mantle are consistent with the presence of garnet (Hood and Jones, 1987; Kuskov and Fabrichnaya, 1994). Recent trace element analysis of lunar volcanic glass beads (Neal, 2001) suggests they may have been derived from garnet-bearing primitive mantle. In addition, Hf isotope data from high and low Ti mare basalts (Unruh et al., 1984; Beard et al., 1998) can be explained by melting out of a garnet-bearing mantle. None of the samples analyzed and corrected for cosmogenic-produced ^{182}W, however, are thought to have formed in such an environment, so a detailed assessment is left for future studies. Future work could try to identify ^{182}W enrichments in lunar samples thought to be derived from such deep garnet-bearing mantle, either through coordinated analysis of samples for multiple isotopes, or analysis that complements previous studies.

Among the SNC meteorites, there is a negative correlation between ε_W and ε_{Nd} and γ_{Os} (Brandon et al., 2000), which is difficult to evaluate because we have limited partitioning data for Re and Os. Rhenium is compatible in garnet (Righter and Hauri, 1998), but if it were more compatible than Os, one might expect a positive correlation between ε_W, ε_{Nd} and γ_{Os}. The correlation with γ_{Os} could also be due to a phase such as clinopyroxene or spinel-structured oxide. Alternatively, the correlation with γ_{Os} may be due to core formation and metal silicate partitioning in which Re and Os are fractionated to non-chondritic ratios in portions of the Martian mantle. Evaluation of these possibilities awaits further partitioning studies and perhaps analyses of ε_{Hf} in nakhlites and Chassigny.

Acknowledgments—This work is supported by NASA grant NAG5-9435. Ken Domanik provided assistance on the electron microprobe. Discussions with D.-C. Lee, A. N. Halliday, A. Brandon, R. J. Walker, M. J. Drake, Q. Yin, and H. Palme over the last few years have influenced this work. This manuscript also benefitted from the journal reviews of R. J. Walker, D. C. Lee and A. D. Brandon and comments of C. Neal.

Associate editor: C. R. Neal

REFERENCES

Alibert C., Michard A., and Albarede F. (1986) Isotope and trace element geochemistry of Colorado Plateau volcanics. *Geochim. Cosmochim. Acta* **50,** 2735–2750.

Beard B. L., Taylor L. A., Scherer E. E., Johnson C. M., and Snyder G. A. (1998) The source region and melting mineralogy of high-titanium and low titanium lunar basalts deduced from Lu-Hf isotope data. *Geochim. Cosmochim. Acta* **62,** 525–544.

Bertka C. M. and Fei Y. (1997) Mineralogy of the martian interior up to core-mantle boundary pressures. *J. Geophys. Res.* **102,** 5251–5264.

Blichert-Toft J., Gleason J. D., Telouk P., and Albarede F. (1999) The Lu-Hf geochemistry of shergottites and the evolution of the martian mantle-crust system. *Earth Planet. Sci. Lett.* **173,** 25–39.

Borg L. E., Nyquist L. E., Taylor L. A., Wiesmann H., and Shih C.-Y. (1997) Constraints on Martian differentiation processes from Rb-Sr and Sm-Nd isotopic analyses of the basaltic shergottite QUE 94201. *Geochim. Cosmochim. Acta* **61,** 4915–4931.

Brandon A. D., Walker R. J., Morgan J. W., and Goles G. G. (2000) Re-Os isotopic evidence for early differentiation of the martian mantle. *Geochim. Cosmochim. Acta* **64,** 4083–4095.

Carlson R. W. and Lugmair G. W. (2000) Timescales of planetesimal formation and differentiation based on extinct and extant radioisotopes. In *Origin of the Earth and Moon* (eds. R. M. Canup and K. Righter), pp. 25–44. University of Arizona Press, Tucson..

Chen C.-Y., Frey F. A., and Garcia M. O. (1990) Evolution of alkalic lavas at Haleakala Volcano, East Maui, Hawaii. *Contrib. Mineral. Petrol.* **105,** 197–218.

Davies G. F. (1990) Heat and mass transport in the early Earth. In *The Origin of the Earth* (eds. H. Newsom and J. H. Jones), pp. 175–194. Oxford University Press, London.

Dreibus G. and Wänke H. (1980) The bulk composition of the eucrite parent asteroid and its bearing on planetary evolution. *Z. Naturforsh.* **35a,** 204–216.

Dunn T. (1987) Partitioning of Hf, Lu, Ti and Mn between olivine, clinopyroxene and basaltic liquid. *Contrib. Mineral. Petrol.* **96,** 476–484.

Elkins-Tanton L. T., van Orman J. A., Hager B. H., and Grove T. L. (2002) Re-examination of the lunar magma ocean cumulate overturn hypothesis: Melting or mixing is required. *Earth Planet. Sci. Lett.* **196,** 239–249.

Ertel W., O'Neill H. S., Dingwell D. B., and Spettel B. (1996) Solubility of tungsten in a haplobasaltic melt as a function of temperature and oxygen fugacity. *Geochim. Cosmochim. Acta* **60,** 1171–1180.

Frey F. A. and Prinz M. (1978) Ultramafic inclusions from San Carlos, Arizona: Petrologic and geochemical data bearing on their petrogenesis. *Earth Planet. Sci. Lett.* **38,** 129–176.

Halliday A. N., Wanke H., Birck J.-L., and Clayton R. N. (2001) The accretion, compositon and early differentiation of Mars. *Space Sci. Rev.* **96,** 197–230.

Harper C. L. Jr. and Jacobsen S. B. (1996) Evidence for ^{182}Hf in the early solar system and constraints on the timescale of terrestrial acccretion and core formation. *Geochim. Cosmochim. Acta* **60,** 1131–1153.

Harper C. L. Jr., Nyquist L. E., Bansal B., Wiesmann H., and Shih C.-Y. (1995) Rapid accretion and early differentiation of Mars indicated by ^{142}Nd/^{144}Nd in SNC meteorites. *Science* **267,** 213–217.

Hart S. R. and Dunn T. (1993) Experimental cpx/melt partitioning of 24 trace elements. *Contrib. Mineral. Petrol.* **113,** 1–8.

Hasenaka T. and Carmichael I. S. E. (1987) The cinder cones of Michoacń-Guanajuato, central Mexico: Petrology and chemistry. *J. Petrol.* **28,** 241–69.

Hauri E. H., Wagner T. P., and Grove T. L. (1994) Experimental and natural partitioning of Th, U, Pb and other trace elements between garnet, clinopyroxene and basaltic melts. *Chem. Geol.* **117,** 149–166.

Herd C. D. K., Borg L. E., Jones J. H., and Papike J. J. (2002) Oxygen fugacity and geochemical variations in the martian basalts: Implications for martian basalt petrogenesis and the oxidation state of the upper mantle of Mars. *Geochim. Cosmochim. Acta* **66,** 2025–2036.

Hess P. C. and Parmentier E. M. (1995) A model for the thermal and chemical evolution of the Moon's interior: Implications for the onset of mare volcanism. *Earth Planet. Sci. Lett.* **134,** 501–514.

Hill E., Wood B. J., and Blundy J. D. (2000) The effect of Ca-Tschermaks component on trace element partitioning between clinopyroxene and silicate melt. *Lithos* **53,** 203–215.

Hillgren V. J. (1991) Partitioning behavior of Ni, Co, Mo, and W between basaltic liquid and Ni-rich metal—Implications for the origin of the moon and lunar core formation. *Geophys. Res. Lett.* **18,** 2077–2080.

Holloway J. R., Pan V., and Gudmundsson G. (1992) High-pressure fluid-absent melting experiments in the presence of graphite: Oxygen fugacity, ferric/ferrous ratio and dissolved CO_2. *Eur. J. Mineral.* **4,** 105–114.

Hood L. L. and Jones J. H. (1987) Geophysical constraints on lunar bulk composition and structure: A reassessment. *J. Geophys. Res.* **92**(Suppl.), E396–E410.

Hood L. L. and Zuber M. T. (2000) Recent refinements in geophysical constraints on lunar origin and evolution. In *Origin of the Earth and Moon* (eds. R. M. Canup and K. Righter), pp. 397–410. University of Arizona Press, Tucson.

Ida S., Canup R. M., and Stewart G. R. (1997) Lunar accretion from an impact-generated disk. *Nature* **389,** 353–57.

Jaeger W. L. and Drake M. J. (2000) Solubilities of W, Ga and Co in silicate melts as a function of melt composition. *Geochim. Cosmochim. Acta* **64,** 3887–3895.

Jarosewich E. (1990) Chemical analyses of meteorites: A compilation of stony and iron meteorite analyses. *Meteoritics* **25,** 323–337.

Kleine T., Munker C., Mezger K., and Palme H. (2002) Rapid accretion and early core formation on asteroids and the terrestrial planets from Hf–W chronometry. *Nature* **418,** 952–955.

Kuskov O. L. and Fabrichnaya O. B. (1994) Constitution of the Moon, 2. composition and seismic properties of the lower mantle. *Phys. Earth Planet. Int.* **83,** 197–213.

Lee D.-C. and Halliday A. N. (1997) Core formation on Mars and differentiated asteroids. *Nature* **388,** 854–857.

Lee D.-C., Halliday A. N., Snyder G. A., and Taylor L. A. (1997) The age and origin of the Moon. *Science* **278,** 1098–1103.

Lee D.-C., Halliday A. N., Leya I., and Weiler R. (2001) Cosmogenic tungsten on the Moon. *Meteoritics Planet. Sci.* **36,** A111.

Lee D.-C., Halliday A. N., Leya I., Wieler R., and Wiechert U. (2002) Cosmogenic tungsten and the origin and earliest differentiation of the Moon. *Earth Planet. Sci. Lett.* **198,** 267–274.

Leya I., Wieler R., and Halliday A. N. (2000) Cosmic-ray production of tungsten isotopes in lunar samples and meteorites and its implications for Hf-W cosmochemistry. *Earth Planet. Sci. Lett.* **175,** 1–12.

Longhi J., Knittle E., Holloway J. R., and Wänke H. (1992) The bulk composition, mineralogy and internal structure of Mars. In *Mars* (eds. H. H. Kieffer, B. M. Jakosky, C. W. Snyder, and M. S. Matthews), pp. 184–208. University of Arizona Press, Tucson.

Lundstrom C. C., Shaw H. F., Ryerson F. J., Williams Q., and Gill J. (1998) Crystal chemical control of clinopyroxene-melt partitioning in the Di-Ab-An system: Implications for elemental fractionation in the depleted mantle. *Geochim. Cosmochim. Acta* **62,** 2849–2862.

McKay G. A and Le L. (1999) Partitioning of W and Hf between ilmenite and mare basaltic melt. *Lunar Planet. Sci.* **30,** abstract #1996.

McKay G. A., Wagstaff J., and Yang S.-R. (1986) Zr, Hf, and REE partition coefficients for ilmenite and other minerals in high-Ti lunar basalts: An experimental study. In *Proc. Lunar Planet. Sci. Conf. 16th*, pp. 229–237.

Myers J. and Eugster H. (1983) The system Fe-Si-O: Oxygen buffer calibrations to 1500 K. *Contrib. Mineral. Petrol.* **82,** 75–85.

Neal C. R. (2001) Interior of the Moon: The presence of garnet in the primitive deep lunar mantle. *J. Geophys. Res. Planets* **106,** 27865–27886.

Newsom H. E. (1995) Composition of the solar system, planets, meteorites, and major terrestrial reservoirs. In *Global Earth Physics: A Handbook of Physical Constants: AGU Reference Shelf*, Vol. 1 (ed. T. J. Ahrens), pp. 159–189. American Geophysical Union, Washington, DC.

Newsom H. and Drake M. J. (1982) The metal content of the eucrite parent body: Constraints from the partitioning behavior of tungsten. *Geochim. Cosmochim. Acta* **46,** 2483–2489.

Newsom H. E., Sims K. W. W., Noll P. D. Jr., Jaeger W. L., Maehr S. A., and Beserra T. B. (1996) The depletion of tungsten in the bulk silicate earth: Constraints on core formation. *Geochim. Cosmochim. Acta* **60,** 1155–1169.

Nixon P. H. (1987) *Mantle Xenoliths*. John Wiley, New York.

Nyquist L. E., Wiesmann H., Bansal B., Shih C.-Y., Keith J. E., and Harper C. L. Jr. (1995) ^{146}Sm-^{142}Nd formation interval for the lunar mantle. *Geochim. Cosmochim. Acta* **59,** 2817–2837.

Palme H. and Wanke H. (1975) A unified trace element model for the evolution of the lunar mantle and crust. In *Proc. Lunar Sci. Conf. 6th*, pp. 1179–1202.

Palme H., and Rammensee W. (1981) The significance of W in planetary differentiation processes; evidence from new data on eucrites. In *Proc. Lunar Planet. Science Conf. 12th*, Part B, pp. 949–964.

Patchett P. J. (1983) Importance of the Lu-Hf isotopic system in studies of planetary chronology and chemical evolution. *Geochim. Cosmochim. Acta* **47,** 81–91.

Righter K. (2002) Does the Moon have a metallic core? Constraints from giant impact modelling and siderophile elements. *Icarus* **158,** 1–13.

Righter K. and Carmichael I. S. E. (1993) Mega-xenocrysts in alkali-olivine basalts: Fragments of disrupted mantle assemblages. *Am. Mineral.* **78,** 1230–1245.

Righter K. and Drake M. J. (1996) Core formation in Earth's Moon, Mars and Vesta. *Icarus* **124,** 513–529.

Righter K. and Hauri E. H. (1998) Compatibility of rhenium in garnet during mantle melting and magma genesis. *Science* **280,** 1737–1741.

Righter K. and Drake M. J. (1999) Effect of water on metal-silicate partitioning of siderophile elements: A high pressure and temperature terrestrial magma ocean and core formation. *Earth Planet. Sci. Lett.* **171,** 383–399.

Righter K. and Drake M. J. (2000) Metal-silicate equilibrium in the early Earth: New constraints from volatile moderately siderophile elements Ga, Sn, Cu and P. *Geochim. Cosmochim. Acta* **64,** 3581–3597.

Righter K., Drake M. J., and Yaxley G. (1997) Prediction of siderophile element metal – silicate partition coefficients to 120 kb and 2800 °C: The effect of pressure, temperature, fO_2 and silicate and metallic melt composition. *Phys. Earth Planet. Int.* **100,** 115–134.

Righter K., Hervig R. L., and Kring D. (1998) Accretion and core formation in Mars: Molybdenum contents of melt inclusion glasses from three SNC meteorites. *Geochim. Cosmochim. Acta* **62,** 2167–2177.

Salters V. J. M. and Longhi J. (1998) Trace element partitioning during the initial stages of melting beneath mid-ocean ridges. *Earth Planet. Sci. Lett.* **166,** 15–30.

Schoenberg R., Kamber B. S., Collerson K. D., and Eugster O. (2002) New W-isotope evidence for rapid terrestrial accretion and very early core formation. *Geochim. Cosmochim. Acta* **66,** 3151–3160.

Shearer C. K. and Papike J. J. (1999) Magmatic evolution of the Moon. *Am. Mineral.* **84,** 1469–1494.

Shearer C. K. and Newsom H. E. (2000) W-Hf isotope abundances and the early origin and evolution of the Earth-Moon system. *Geochim. Cosmochim. Acta* **64,** 3599–3613.

Skulski T., Minarik W., and Watson E. B. (1994) High-pressure experimental trace-element partitioning between clinopyroxene and basaltic melts. *Chem. Geol.* **117,** 127–147.

Snyder D. A. and Carmichael I. S. E. (1992) Olivine-liquid equilibria and the chemical activities of FeO, NiO, Fe_2O_3, and MgO in natural basic melts. *Geochim. Cosmochim. Acta* **56,** 303–318.

Snyder G. A., Taylor L. A., and Neal C. R. (1992) A chemical model for generating the sources of mare basalts: Imperfect, geologically realistic fractional crystallization of the lunar magmasphere. *Geochim. Cosmochim. Acta* **56,** 3809–3823.

Solomon S. C and Longhi J. (1977) Magma oceanography: 1. Thermal evolution. In *Proc. Lunar Planet. Sci. Conf. 8th*, pp. 583–599.

Solomotov V. S. (2000) Fluid dynamics of a terrestrial magma ocean. In *Origin of the Earth and Moon* (eds. R. M. Canup and K. Righter), pp. 323–338. University of Arizona Press, Tucson.

Spera F. J. (1992) Lunar magma transport phenomena. *Geochim. Cosmochim. Acta* **56,** 2253–2266.

Taylor J. R., Wall V. J., and Pownceby M. I. (1992) The calibration and application of accurate redox sensors. *Am. Mineral.* **77,** 284–295.

Unruh D. M., Stille P., Patchett P. J., and Tatsumoto M. (1984) Lu-Hf and Sm-Nd evolution in lunar mare basalts. *J. Geophys. Res.* **89**(Suppl.), B459–B477.

van Orman J. A. and Grove T. L. (2000) Origin of lunar high-titanium ultramafic glasses: Constraints from phase relations and dissolution kinetics of clinopyroxene-ilmenite cumulates. *Met. Planet. Sci.* **35,** 783–794.

van Westrenen W., Blundy J. P., and Wood B. J. (1999) Crystal chemical controls on trace element partitioning between garnet and anhydrous silicate melt. *Am. Mineral.* **84,** 838–847.

van Westrenen W., Blundy J. P., and Wood B. J. (2001) High field strength element/rare earth element fractionation during partial melting in the presence of garnet: Implications for identification of mantle heterogeneities. *Geochem. Geophys. Geosys.* **2,** paper 2000GC000133.

Wadwha M. (2001) Redox state of Mars' upper mantle and crust from Eu anomalies in shergottite pyroxenes. *Science* **291,** 1527–1530.

Walter M. J., Newsom H., Ertel W., and Holzheid A. (2000) Siderophile elements in the Earth and Moon: Metal/silicate partitioning and implications for core formation. In *Origin of the Earth and Moon* (eds. R. M. Canup and K. Righter), pp. 265–290. University of Arizona Press, Tucson.

Warren P. H. (1985) The magma ocean concept and lunar evolution. *Ann. Rev. Earth Planet. Sci.* **13,** 201–240.

Watson E. B., BenOthman D., Luck J.-M., and Hofmann A. W. (1987) Partitioning of U, Pb, Cs, Yb, Hf, Re, and Os between chromian diopsidic pyroxene and haplobasaltic liquid. *Chem. Geol.* **62,** 191–208.

Yin Q., Jacobsen S. B., Yamashita K., Blichert-Toft J., Telouk P., and Albarede F. (2002) A short timescale for terrestrial planet formation from Hf–W chronometry of meteorites. *Nature* **418,** 949–952.